Characterization of Cation-Binding Sequences in the Platelet Integrin GPIIb-IIIa ($\alpha_{IIb}\beta_3$) by Terbium Luminescence†

Czeslaw S. Cierniewski,‡ Thomas A. Haas,‖ Jeffrey W. Smith,§ and Edward F. Plow*,‖

Department of Biophysics, Medical University in Lodz, Lodz, Poland, Department of Vascular Biology, The Scripps Research Institute, La Jolla, California 92037, and Center for Thrombosis and Vascular Biology, Cleveland Clinic Foundation/FF20, 9500 Euclid Avenue, Cleveland, Ohio 44195

Received January 31, 1994; Revised Manuscript Received August 2, 1994®

ABSTRACT: The binding of cations to purified GPIIb-IIIa ($\alpha_{IIb}\beta_3$) and synthetic peptides corresponding to the potential cation-binding sites within this integrin has been assessed by terbium luminescence spectroscopy. Tb^{3+} supported fibrinogen binding to purified GPIIb-IIIa, at lower concentrations than Ca^{2+}, consistent with its higher affinity for cation-binding motifs. Titration analyses indicated the presence of five Tb^{3+}-binding sites of relatively high affinity in the receptor. These sites also could be filled by divalent cations. Six sequences within GPIIb-IIIa have the appropriate spacing of five of the usual six coordination sites for cations in functional Ca^{2+}-binding EF-hand motifs. Peptides containing Tyr and/or Trp at selected positions as fluorescence energy donors were synthesized, and their Tb^{3+}-binding capacity was assessed. The four potential Ca^{2+}-binding sequences in the GPIIb subunit, GPIIb 242–255, 296–309, 364–377, and 425–438, were functional, despite lacking the usual Glu residue at the terminal coordination position. These peptides bound Tb^{3+} with the same affinity as typical Ca^{2+}-binding loop peptides and also bound Ca^{2+} and other divalent cations without preference. Of the two candidate GPIIIa sequences, 118–131 and 208–221, the former bound Tb^{3+} and divalent cations with an affinity similar to that of the GPIIb peptides, whereas the latter peptide was not functional. This functional difference, as well as data obtained with substituted peptides, emphasizes the importance of the first coordination position for interaction of synthetic peptide loops with cations. Together, these data identify the five cation-binding sites within intact GPIIb-IIIa.

GPIIb-IIIa ($\alpha_{IIb}\beta_3$), a member of the integrin family of cell-surface receptors (Hynes, 1987; Plow & Ginsberg, 1989; Phillips et al., 1988), consists of two nonidentical, noncovalently associated subunits, GPIIb and GPIIIa. Divalent cations are required to maintain the association between the subunits (Fujimura & Phillips, 1983; Brass et al., 1985; Fitzgerald & Phillips, 1985; Steiner et al., 1989), to determine the conformation of the heterodimeric complex (Steiner et al., 1991; Ginsberg et al., 1986), and to support the ligand-binding functions of this receptor for adhesive proteins such as fibrinogen (Marguerie et al., 1980; Kirchhofer et al., 1990). Indeed, ligand binding to all integrins is cation-dependent (Ruoslahti, 1991; Smyth et al., 1993). Equilibrium dialysis (Rivas & González-Rodríguez, 1991) and *in situ* cobalt oxidation studies (Piotrowicz et al., 1991) have suggested the presence of approximately five metal ion binding sites within GPIIb-IIIa. Consistent with this number, inspection of the primary structures of the subunits identifies four to six stretches of 12 contiguous amino acids which resemble EF-hand Ca^{2+}-binding motifs (Fitzgerald et al., 1987; Poncz et al., 1987). In calmodulin and other Ca^{2+}-binding proteins with functional EF-hands, the 12 amino acids form a loop which is flanked by α-helices. Functional EF-hands conform to a consensus sequence, X-2-Y-4-Z-6-(-Y)-8-(-X)-10-11-(-Z), in which the numbers identify the positions of the 12 amino acids within the loop and X, Y, and Z are oxygenated residues which coordinate Ca^{2+} (Strynadka & James, 1989). Asp is the preferred residue at the X position, Glu is preferred at the -Z position, and Gly is most usually found at the sixth position, between Z and -Y. Not one of the candidate sequences within either subunit of GPIIb-IIIa conforms precisely to these specifications.

The candidate cation-binding sequences within GPIIb are GPIIb 242–255, 296–309, 364–377, and 425–438. These lack a suitable coordinating residue at the -Z position and do not appear to be flanked by helical segments. To what extent these deviations impair Ca^{2+}-binding function is uncertain. However, computer modeling of the putative Ca^{2+}-binding loops within integrin α-chains suggests that they could resemble conventional EF-hands (Tuckwell et al., 1992). Moreover, a recombinant protein corresponding to GPIIb 171–464 (containing the four putative Ca^{2+}-binding motifs) was capable of binding divalent ions (Gulino et al., 1992). These data suggest that one or more of the four EF-hand-like sequences in GPIIb is a functional metal-binding site.

The candidate cation-binding sequences in GPIIIa are GPIIIa 118–131 and 208–221. GPIIIa 118–131 lacks a suitable coordination residue at the -Z position and has a Met, rather than a Gly, at the sixth position. While GPIIIa 208–221 has Glu at the -Z position and is the only GPIIb-IIIa sequence to have this preferred residue at this position, it lacks Asp at the X position and has a bulky Arg at the sixth position. The evidence to suggest that these two GPIIIa sequences have metal-binding function is only inferential. Naturally occurring mutations in these sequences render the receptor nonfunctional (Loftus et al., 1990; Bajt et al., 1992; Lanza et al., 1992); since ligand and metal binding are intimately linked in integrins, it follows that these sequences may be involved in cation binding.

The utility of lanthanide luminescence spectroscopy as a probe of the solution structure of Ca^{2+}- and other cation-

† This work was supported in part by NIH Grant HL-38292.
* To whom correspondence should be addressed.
‡ Medical University in Lodz.
§ The Scripps Research Institute.
‖ Cleveland Clinic Foundation/FF20.
® Abstract published in *Advance ACS Abstracts,* September 15, 1994.

0006-2960/94/0433-12238$04.50/0

binding proteins is well established [e.g., Horrocks and Sudnick (1981), Horrocks and Albin (1983), and Reuken (1977)]. Terbium(III) (Tb^{3+}) luminescence spectroscopy has been applied to a number of proteins in which Ca^{2+} plays a role in tertiary stabilization (Snyder et al., 1981), quaternary structure (Burroughs et al., 1992), conformational regulation (van Sharrenberg et al., 1985), or catalytic action (Babu et al., 1985). This technique also allows discrimination among Ca^{2+}-binding sites of differing affinities and permits calculation of absolute and relative binding constants of both intact proteins and synthetic peptides for metal ions (Burroughs et al., 1992). Tb^{3+} and Ca^{2+} have ionic radii of about 1 Å, coordination numbers between 6 and 8, and a preference for coordination with oxygen rather than nitrogen atoms. However, due to its higher charge density, Tb^{3+} can substitute with higher affinity than Ca^{2+} in many Ca^{2+}-binding proteins (Prados et al., 1974). The quantum yield of luminescence is extremely low for free Tb^{3+} but increases upon its binding in close proximity to aromatic groups within proteins or peptides (Luk, 1971). Under this circumstance, when the liganding protein is irradiated in the vicinity of its Phe, Tyr, or Trp ultraviolet absorption bands, the luminescence of bound Tb^{3+} is enhanced as a result of energy transfer. This phenomenon appears to occur generally, and enhanced Tb^{3+} luminescence has been observed in over 90% of the Ca^{2+}-binding proteins tested (Brittain et al., 1976).

In this study, we have used Tb^{3+} luminescence spectroscopy to characterize the interaction of divalent cations with GPIIb-IIIa and its candidate metal-binding sequences. Peptides corresponding to the putative Ca^{2+}-binding sites within both subunits have been synthesized and assessed for cation binding. This approach has been successfully used in studies of EF-hand-like sites of troponin C (Kanellis et al., 1983; Malik et al., 1987) and proteins of the calmodulin family (MacManus et al., 1990).

EXPERIMENTAL PROCEDURES

GPIIb-IIIa Preparation. GPIIb-IIIa was isolated from outdated platelets by RGD affinity chromatography (Pytela et al., 1986). Briefly, platelets were lysed in buffer containing 10 mM Hepes, 150 mM NaCl, 1 mM $CaCl_2$, 1 mM $MgCl_2$, 0.1 mM leupeptin, 10 mM *N*-ethylmaleimide, 1 mM phenylmethanesulfonyl fluoride, and 50 mM octyl glucoside, pH 7.3, centrifuged for 1 h at 30000*g*, and applied onto GRGDSPK–Sepharose (column, 12 × 2.5 cm). The affinity matrix was equilibrated with the lysis buffer. Detergent extracts of platelet proteins were recycled over the affinity matrix at a flow rate of 0.5 mL/min at 4 °C. Unbound proteins were eluted with 10 column volumes of column buffer, identical to lysis buffer except that the octyl glucoside content was lowered to 25 mM. Proteins remaining bound onto the RGD affinity matrix were eluted with buffer containing RGDF (1 mg/mL). Fractions were analyzed by electrophoresis on 7% polyacrylamide gels in SDS under nonreducing conditions (Laemmli, 1970). Prior to spectrofluorometric measurements, samples of GPIIb-IIIa were dialyzed against either 50 mM MOPS, pH 7.3, containing 0.1% CHAPS or 50 mM PIPES, pH 6.5, containing 0.1% CHAPS. When GPIIb-IIIa was recycled over the GRGDSPK–Sepharose column in these buffer systems, it was still bound and eluted with free peptide, indicating that the receptor retained ligand-binding function in CHAPS. All buffers were treated with CHELEX 100 (Bio-Rad Laboratories, Richmond, CA).

Peptide Synthesis and Purification. Peptides were synthesized in an Applied Biosystems Model 431 peptide synthesizer (Foster City, CA) using 9-fluoronylmethoxycarbonyl chemistry. Peptides were subsequently applied to a reverse-phase Syn-Chropak RPP (250 × 4.1 mm) column, equilibrated in 0.1% trifluoroacetic acid, and eluted with a gradient of acetonitrile (1%/min for 50 min at a flow rate of 1 mL/min). Stock solutions of lyophilized peptides were prepared for spectroscopy in water derived from a Milli Q purification system (Millipore, Bedford, MA). The concentrations of the peptide solutions were determined spectrophotometrically using an extinction coefficient of 1490 $M^{-1}cm^{-1}$ at 276 nm or 4850 M^{-1} cm^{-1} at 289 nm for Tyr and Trp, respectively. For these measurements, the peptides were dissolved in 6 M guanidine HCl. Peptide purity was assessed by reverse-phase HPLC and by amino acid sequence analysis. Before use, the purified peptides in water were diluted to an absorbance at 285 nm of 0.10 and to a final concentration of 10 mM HEPES buffer, pH 7.3.

Circular dichroism (CD) measurements were performed on a JASCO Model J600 spectropolarimeter fitted with a thermally regulated cell holder in 1-mm rectangular quartz cuvettes. The CD spectra of the peptides dissolved in 50 mM NaCl and 2 mM HEPES, pH 7.0, with or without 50% trifluoroethanol were analyzed from 250 to 200 nm, every 0.5 nm, with 2-s collection times. In a comparison of the CD spectra of the peptides corresponding to the naturally occurring sequences in GPIIb and GPIIIa with those of peptides with aromatic amino acid substitutions to facilitate fluorescence energy transfer (see below), no significant difference in percentage of ordered structure, as estimated by their ellipticity at 208 and 222 nm, was observed. All peptides had >70% unordered structure, and the variant peptides displayed secondary structures similar to the native peptides. The only peptide set showing a slight difference in CD spectra was that corresponding to $IIb_{242-255}$; the substituted peptide ($IIb_{242-253}$: GEFDGDLYTTEWVV) showed a slight increase in helical content (6% vs 2%) compared to the native sequence peptide ($IIb_{242-253}$:GEFDGDLNTTEYVV).

Tb^{3+} Binding to GPIIb-IIIa and Synthetic Peptides. The highest available grades of terbium chloride ($TbCl_3$) hexahydrate were obtained from Aldrich and used without further purification. Stock solutions of $TbCl_3$ (100 mM) were dissolved in water and were standardized by titration with EDTA at pH 6.0, employing Arsenazo III as the indicator.

Tb^{3+} binding to GPIIb-IIIa and synthetic peptides was assessed at 20 °C using two different methods that gave essentially identical results. The first method was used at pH 7.3; individual samples for each point on the titration curve were incubated overnight at 4 °C before making the luminescence measurements. The second method was used at pH 6.5; successive additions of Tb^{3+} were made to a single GPIIb-IIIa or peptide sample, and measurements were made after 5–10 min. With some peptides, a precipitate developed when the ratio of Tb^{3+} to peptide exceeded 3:1. Therefore, all titrations were conducted at or below this ratio. Similarly, aggregation of GPIIb-IIIa, evaluated by turbidimetric measurements at 400 nm and by HPLC analysis on a TSK-4000 column, was observed when Tb^{3+} was added to a final concentration of 20 μM; thus, all reported experiments with the intact receptor were performed below this concentration. In preliminary experiments the effect of different detergents (octyl glucoside, CHAPS, Triton X-100, Tween 20) on intrinsic fluorescence and terbium luminescence of GPIIb-IIIa was tested. Essentially identical terbium titration curves were obtained when GPIIb-IIIa was used in buffers containing octyl

glucoside and CHAPS. However, background fluorescence was lower in CHAPS, and this detergent was used in all subsequent experiments. Binding isotherms of Tb^{3+} to GPIIb-IIIa in CHAPS were analyzed using the Sigmaplot curve fitting program.

To assess the relationship between the Tb^{3+}- and divalent cation-binding sites, the reduction in emission intensity at 545 nm was determined upon the addition of aliquots of 50 mM solutions of $CaCl_2$, $MgCl_2$, or $MnCl_2$ to GPIIb-IIIa or peptides equilibrated with a known concentration of Tb^{3+}. In experiments where Tb^{3+} was excited by energy transfer from Trp or Tyr residues, Tb^{3+}, Ca^{2+}, or other ions were added in microliter amounts not exceeding 100 μL to a starting volume of 1.5 mL. The displacement of Tb^{3+} from GPIIb-IIIa by Mn^{2+} was analyzed using the Sigmaplot program, fitting the experimental data to the following equation:

$$B = \sum_i \frac{n_i[Mn^{2+}]/K_{di}}{1 + [Mn^{2+}]/K_{di}}$$

where B is the moles of bound Mn^{2+} per mole of protein, n is the number of Mn^{2+}-binding sites of each class, $[Mn^{2+}]$ is the concentration of free Mn^{2+}, and K_{di} is the dissociation constant of the ith class.

The binding constants of the peptides with Tb^{3+} were calculated from the following equation: $K_a = v/\{(1 - v)(R - v)[P]_0\}$, where $R = [Tb^{3+}]_{tot}/[P]_0$, $v = F/F_0$ (v, relative change of fluorescence intensity at a given R, at fixed wavelength), and $[Tb^{3+}]_{tot}$ and [P]0 are the total concentrations of Tb^{3+} and peptide, respectively (Borin et al., 1989). The binding constants of Ca^{2+}, Mg^2, and Mn^{2+} were calculated from competitive binding experiments in which $[P]_0 = 20$ μM, $[Tb^{3+}]_{tot} = 15$ μM, and the ratios $[Ca^{2+}]_{tot}/[Tb^{3+}]_{tot}$, $[Mg^{2+}]_{tot}/[Tb^{3+}]_{tot}$, and $[Mn^{2+}]_{tot}/[Tb^{3+}]_{tot}$ are the values at which 50% of the total fluorescence change occurred. Assuming that $[Ca^{2+}]_f = [Ca^{2+}]_{tot}$ and $[Tb^{3+}]_f = [Tb^{3+}]_{tot} - 0.5[P]_0$, then the concentration of metal (Me) complex is equal to that of Tb^{3+} complex and $K_{Tb}/K_{Me} = [Me^{2+}]_f/[Tb^{3+}]_f$.

Luminescence Emission Measurements. Measurements of enhanced Tb^{3+} luminescence were made with an SLM 500C spectrofluorometer with a refrigerated bath (RMG LAUDA) at 20 °C and an SLM Spectrum Processor SPF-500C, version 2.4. Emission spectra, excitation spectra, and luminescence intensities were taken with 1- and 7.5-nm band passes for the excitation and emission monochromators, respectively. A cutoff filter in the emission beam was used to eliminate second-order wavelength interference.

The excitation wavelength was chosen at 285 nm to minimize the overlap of second-order diffraction (570 nm) with Tb^{3+} emission at 545 nm. Emission spectra were corrected for the blank contribution and the instrument response and normalized to an absorbance of 0.100 at 285 nm in a quartz cell of 1 cm path length. Excitation spectra were recorded at the fluorescence maximum of the intrinsic fluorophores of Tyr (310 nm) and Trp (350 nm) and at the luminescence maximum of Tb^{3+} (545 nm). Excitation and emission spectra were automatically corrected for lamp intensity variations.

Solid-Phase Fibrinogen-Binding Assay. Fibrinogen was radiolabeled with ^{125}I as previously described (Marguerie et al., 1980). The specific radioactivity of [^{125}I]fibrinogen was about 0.2 μCi/μg. In order to quantify the binding of fibrinogen to GPIIb-IIIa treated with different amounts of Tb^{3+} or Ca^{2+}, microtiter wells (IMMULON 2, Removawell strips, Dynatech Laboratories, Chantilly, VA) were coated overnight at 4 °C with 200 μL 50 mM HEPES buffer, pH 7.3, containing 2 μg/mL purified GPIIb-IIIa, 0.15 M NaCl, 1 mM $CaCl_2$, and 1 mM $MgCl_2$. The plates were then washed and postcoated with 1% bovine serum albumin in the same buffer for 1 h at 37 °C, and the wells were exhaustively washed (six times with 200 μL during 1 h) with Ca^{2+}-free 50 mM HEPES buffer, pH 7.3, containing 0.15 mM NaCl. Then, wells were preincubated with 200 μL of the same buffer containing 0–20 μM Tb^{3+} or 0–1 mM Ca^{2+} for 30 min at room temperature, and 200 ng of [^{125}I]fibrinogen in 20 μL was added to each well. Binding of fibrinogen was determined by direct γ counting of the plastic wells. Nonspecific binding was defined as the residual binding in the presence of a 100-fold excess of nonlabeled fibrinogen or in the presence of 5 mM EDTA and was subtracted from the total binding to generate specific binding values. While the fibrinogen-binding data shown in this study was obtained in the absence of detergent, we also evaluated the effects of 0.1% CHAPS, the detergent used in the luminescence studies, on the interaction. [^{125}I]Fibrinogen binding to the immobilized receptor in the presence of CHAPS was reduced by only 25% compared to that observed in the absence of detergent. This binding remained specific (it was inhibited by nonlabeled fibrinogen and EDTA) and was slightly greater than observed in the presence of 25 mM octyl glucoside.

RESULTS

Tb^{3+} Supports Fibrinogen Binding to GPIIb-IIIa. Initial analyses were performed to determine whether Tb^{3+} would support the ligand-binding function of GPIIb-IIIa in a manner similar to Ca^{2+}. Plastic microtiter wells were coated with purified GPIIb-IIIa, readily dissociable Ca^{2+} was removed by washing, and binding of radioiodinated fibrinogen to the immobilized GPIIb-IIIa was analyzed in the presence of different concentrations of Tb^{3+} or Ca^{2+}. As shown in Figure 1A, Tb^{3+} supported binding of [^{125}I]fibrinogen to GPIIb-IIIa in a concentration-dependent manner; 50% maximal ligand binding was observed at 2.5 μM Tb^{3+}, and maximum binding was attained at 6 μM. These values are considerably lower than those obtained with Ca^{2+} (50% maximal binding required 30 μM Ca^{2+}), consistent with the higher affinity of Tb^{3+} for EF-hand-like Ca^{2+}-binding sites. Fibrinogen binding in the presence of Tb^{3+} exhibited characteristics typical of ligand binding to GPIIb-IIIa in the presence of Ca^{2+} (Figure 1B); namely, binding was inhibited by a γ-chain and a RGD peptide, but not by an RGE peptide, and by an appropriate monoclonal antibody to GPIIb-IIIa.

Interaction of Tb^{3+} with GPIIb-IIIa. With these observations indicating that Tb^{3+} supported the ligand interactions with GPIIb-IIIa, the binding of Tb^{3+} to the receptor was evaluated in detergent solution by using an excitation wavelength of 285 nm, i.e., in the Trp absorption band, and monitoring Tb^{3+} luminescence at 545 nm. The results of three separate titrations of GPIIb-IIIa with Tb^{3+} are shown in Figure 2. The initial component of these titration curves is characterized by a relatively shallow increase in Tb^{3+} emission intensity at Tb^{3+}/GPIIb-IIIa molar ratios of less than 1.0. As additional Tb^{3+} is added, a more pronounced increment in Tb^{3+} luminescence is observed. This increment plateaus at a Tb^{3+}/GPIIb-IIIa ratio of 5.0. Since the quantum yield at a particular Tb^{3+}-binding site is a function of the number of coordinating groups and/or its overall affinity (Horrocks & Sudnick, 1979; Gross et al., 1987), the shape of the titration curve suggests the presence of five Tb^{3+}-binding sites. The dashed line shown in Figure 2 is the theoretical curve calculated for the binding of Tb^{3+} to five sites of equal affinity. The association constant (K_a) used to calculate the theoretical

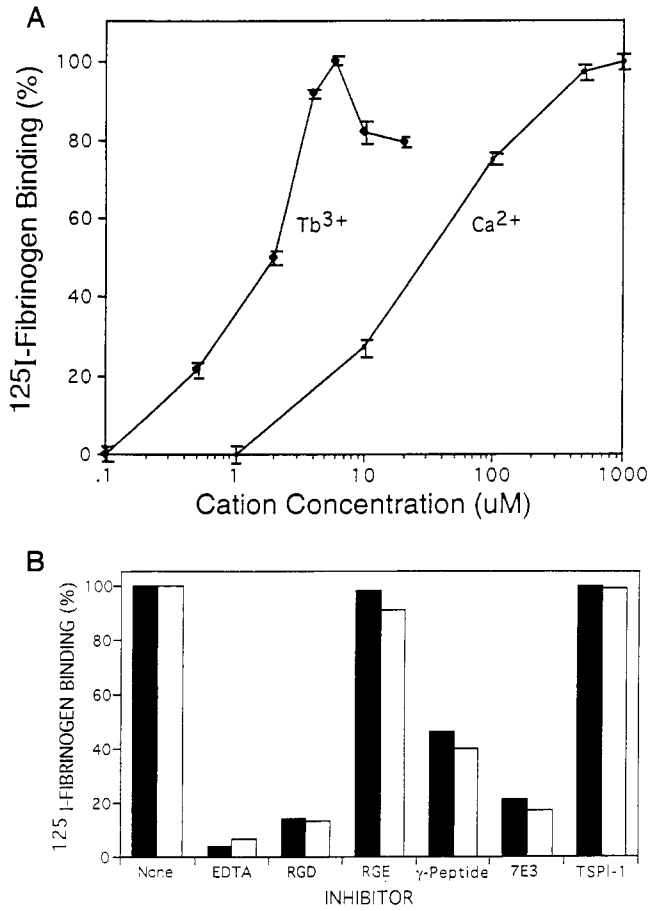

FIGURE 1: (A) Binding of fibrinogen to purified GPIIb-IIIa is supported by Tb^{3+}. GPIIb-IIIa, isolated by RGD affinity chromatography, was coated onto microtiter wells (200 ng/well, overnight at 4 °C), depleted of loosely associated ions by washing with divalent cation-free buffer, and then incubated with 200 ng of [^{125}I]fibrinogen in the presence of 0–20 μM $TbCl_3$ (- ▲ -) or 0–1 mM $CaCl_2$ (- ● -). After binding overnight at 4 °C, unbound fibrinogen was removed by washing, and the wells were counted in a γ counter. Nonspecific binding, defined as the residual [^{125}I]fibrinogen bound in the presence of 5 mM EDTA, was subtracted from total binding to yield specific binding. Maximal binding was calculated relative to the highest specific binding in the presence of Tb^{3+} or Ca^{2+}, and data are means ±SD for three different experiments, each performed in triplicate. (B) Specificity of fibrinogen binding to GPIIb-IIIa in the presence of Tb^{3+}. Inhibitors of fibrinogen binding to GPIIb-IIIa-coated wells are EDTA (5 μM); peptides GRGDSP and GRGESP fibrinogen and the γ-chain peptide, HHLGGAKQAGDV (100μM); and monoclonal antibodies 7E3 to GPIIb-IIIa and TSPI-1 to a control protein, thrombospondin. Results are expressed as percentage of specific binding, defined as the binding inhibited by a 100-fold excess of unlabeled fibrinogen. Fibrinogen binding was performed in the presence of Ca^{2+} (open bars) or Tb^{3+} (shaded bars).

curve was 0.86 μM^{-1}. This K_a value maximized the concordance between the experimental and the theoretical curve. Nevertheless, the experimental data points diverge considerably from the theoretical curve and fit a sigmoidal plot. This divergence indicates that the quantum yields of luminescence obtained upon binding of Tb^{3+} to each of the five sites are not identical. Changes in Tb^{3+} emission above six equivalents could not be investigated because significant aggregation of GPIIb-IIIa occurred at Tb^{3+} concentrations above 20 μM. Such aggregation also has been reported with other proteins (Burroughs et al., 1992; Horrocks & Sudnick, 1981; MacManus et al., 1990).

To determine the relationship between the Tb^{3+}-binding sites and the divalent cation-binding sites within GPIIb-IIIa, displacement of bound Tb^{3+} by Ca^{2+} and Mn^{2+} was analyzed.

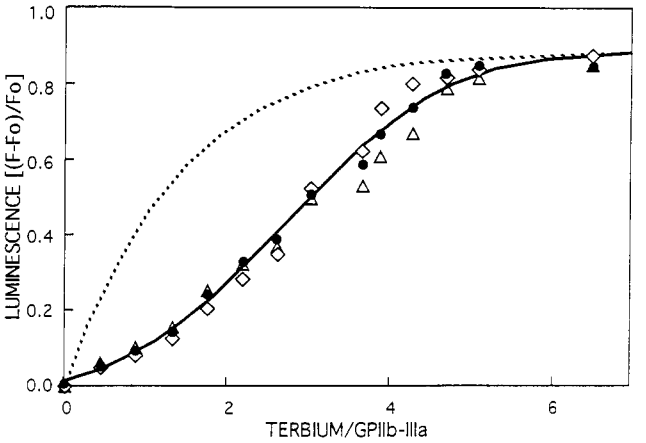

FIGURE 2: Binding of Tb^{3+} to GPIIb-IIIa as monitored by luminescence spectroscopy. Isolated GPIIb-IIIa, in 50 mM MOPS, pH 7.3, containing 0.1% CHAPS, was titrated with $TbCl_3$. Luminescence of Tb^{3+} bound to GPIIb-IIIa was excited by irradiation at 285 nm corresponding to the tryptophan absorption band. Tb^{3+} emission at 545 nm is plotted as a function of the total equivalents of Tb^{3+} added to GPIIb-IIIa. Experimental data points are from three separate experiments. The dashed line is the theoretical fit of five Tb^{3+}-binding sites with the same binding affinity based on the equation $K_a = v/\{(1-v)(R-v)[P]_0\}$. The K_a of the theoretical curve, 0.86 μM^{-1}, maximized the agreement between the experimental and theoretical curves. The solid line through the data points is the best fit using the Sigmaplot computer program to a model in which the site with the highest binding affinity shows lower luminescence than the other four sites upon binding of Tb^{3+}.

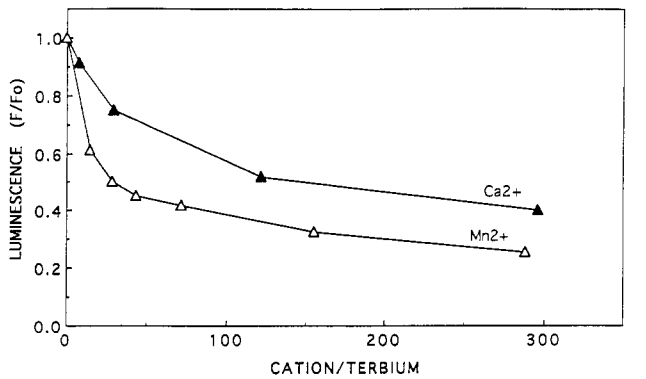

FIGURE 3: Displacement of Tb^{3+} bound to GPIIb-IIIa by Ca^{2+} and Mn^{2+}. Complexes of GPIIb-IIIa and Tb^{3+} (1 μM GPIIb-IIIa and 5 μM $TbCl_3$), in 50 mM MOPS buffer, pH 7.3, containing 0.1% CHAPS, were titrated with $CaCl_2$ (- ▲ -) or $MnCl_2$ (- △ -). Tb^{3+} luminescence was excited at 285 nm and measured at 545 nm.

As shown in Figure 3, the emission intensity of Tb^{3+} bound to GPIIb-IIIa decreased upon addition of either cation. These effects did not arise from changes in the ionic strength of the solvent or in the conformational state in GPIIb-IIIa, as no changes in intrinsic fluorescence were observed upon addition of these divalent ions to the receptor in the absence of Tb^{3+}. Hence, the decrease in emission intensity is attributable to displacement of Tb^{3+} from the receptor by the added cations. To displace 50% of the receptor-bound Tb^{3+}, a 130-fold molar excess of Ca^{2+} or a 30-fold molar excess of Mn^{2+} relative to Tb^{3+} was needed. When Mn^{2+} was added to a final concentration of 2 mM, the decrease in terbium luminescence was 80%, suggesting displacement of approximately four of the five bound terbium ions from GPIIb-IIIa. The experimental data for Tb^{3+} displacement by Mn^{2+} were subjected to nonlinear curve fitting analyses (see Experimental Procedures). The best fit for the binding of Mn^{2+} to these sites was provided by a simple competitive inhibition model for four sites with a single association constant ($K_a = 1.04 \times 10^6\ M^{-1}$).

Table 1: Synthetic GPIIb and GPIIIa Peptides Utilized To Analyze Tb^{3+} Luminescence

			X	2	Y	4	Z	6	-Y	8	-X	10	11	-Z
consensus sequence[a]	G	D	K	D	G	D	G	Y	I	D	F	E	E	L
group 1: GPIIb peptides														
(1) GPIIb 242–255	G	E	F	D	G	D	L	N	T	T	E	Y	V	V
GPIIb 242–255(Y,W)	G	E	F	D	G	D	L	Y	T	T	E	W	V	V
(2) GPIIb 296–309(W)	T	D	V	N	G	D	G	R	H	D	L	W	V	G
GPIIb 296–309(Y,W)	T	D	V	N	G	D	G	Y	H	D	L	W	V	G
(3) GPIIb 364–377(W)	G	D	L	D	R	D	G	Y	N	D	I	W	V	G
(4) GPIIb 425–438(W)	V	D	I	D	D	N	G	Y	P	D	L	W	V	G
group 2: GPIIIa peptides														
(1) GPIIIa 118–131	M	D	L	S	Y	S	M	K	D	D	L	W	S	I
GPIIIa 118–131(A)	M	A	L	S	Y	S	M	K	D	D	L	W	S	I
(2) GPIIIa 208–221(W)	K	K	Q	S	V	S	R	N	R	D	A	W	E	G
GPIIIa 208–221(Y,W)	K	K	Q	S	Y	S	R	N	R	D	A	W	E	G
GPIIIa 208–221(D,Y,W)	K	D	Q	S	Y	S	R	N	R	D	A	W	E	G

[a] The common consensus sequence for the EF-hand Ca^{2+}-binding motif is based on a comparison of about 200 loops. X, Y, and Z refer to the Cartesian positions of the Ca^{2+}-coordinating residues. Group 1, the GPIIb peptides, contain Tyr at position -Y, and group 2, the GPIIIa peptides, contain Tyr at position 4. All peptides contain Trp at position 11.

The K_a for Ca^{2+} in this model was 1.1 μM^{-1}, similar to the calculated K_a for the theoretical curve shown in Figure 2.

Synthesis and Fluorescence Spectroscopy of the Six Candidate Ca^{2+}-Binding Sequences of GPIIb-IIIa. To further characterize the divalent ion-binding properties of the receptor, peptides corresponding to the six candidate Ca^{2+}-binding sequences were synthesized (see Table 1). All peptides were synthesized with the naturally occurring amino acids flanking the twelve amino acids of the EF-hand-like loop. The sequences of all peptides, except GPIIb-IIIa 118–131, were modified by placement of a Trp residue at position 11 in the consensus sequence of an EF-hand loop to facilitate Tb^{3+} luminescence measurements (Trp is naturally occurring at position 11 of two Ca^{2+}-binding motifs in GPIIIa subunit). The validity of this substitution is established by the observations that (1) the amino acid at this position does not contribute to metal binding, i.e., it provides neither coordination sites nor hydrogen bonds to stabilize the configuration of the peptide loop within EF-hands; (2) there is no preference for a particular amino acid residue in this position in functional EF-hands (Hogue et al., 1992; Bairoch, 1989; Tuckwell et al., 1992; Horrocks & Albin, 1983; Snyder et al., 1981; Strynadka & James, 1989); and (3) the CD spectra of the GPIIb and GPIIIa peptides with the natural and the substituted sequences were virtually identical. In order to maximize energy transfer to bound Tb^{3+}, Tyr residues also were placed at position 4 or -Y of some of the peptides; these are the naturally occurring residues in the first Ca^{2+}-binding motif of GPIIIa (GPIIIa 118–131) and the last two Ca^{2+}-binding motifs of GPIIb (GPIIb 364–377 and 425–438). In addition, variant peptide analogues of GPIIIa 118–131 and GPIIIa 208–221 were synthesized. These variants were as follows: (1) an Ala residue, rather than an Asp, was placed at position X of GPIIIa 118–131, the site of the CAM mutation in GPIIb-IIIa (Loftus et al., 1990); (2) an Asp, the preferred residue at position X of EF-hands, was substituted for the Lys at GPIIIa 209. For convenience, the peptides in Table 1 have been divided into GPIIb and GPIIIa peptides. All GPIIb peptides have Tyr at position -Y and Trp at position 11 as potential energy donor residues. All GPIIIa peptides have Tyr at position Y and Trp at position 11 as potential energy donors. Residues within the peptide are identified according to EF-hand nomenclature: X-2-Y-4-Z-6-(-Y)-8-(-X)-10-11-(-Z). Position 1 is X, the first cation coordination site.

In preliminary experiments, the fluorescence emission spectra of all synthetic peptides were analyzed in the 300–600 nm wavelength range using an excitation wavelength of 285 nm in the presence of increasing amounts of Tb^{3+}. The quenching of the Trp emission fluorescence at 350 nm, due to energy transfer from the aromatic chromophore to Tb^{3+}, and the corresponding enhancement in the fluorescence of the cation at 490 and 545 nm were evident for each peptide (not shown). In principle, information on binding of Tb^{3+} and other cations to the peptides can be obtained either from the enhancement of the fluorescence quantum yield of Tb^{3+} at 490 and 545 nm or from the quenching of the Trp emission at 350 nm. However, the relative fluorescence changes at 350 and 490 nm were much smaller than that at 545 nm. Therefore, in all experiments presented, the changes in Tb^{3+} luminescence intensity at 545 nm in the peptide samples, upon excitation at 285 nm, were analyzed.

Under these conditions, energy transfer to Tb^{3+} occurred from both aromatic amino acid residues, Trp and Tyr. As evidenced by the experiments shown in Figure 4, the contribution of the Tyr residue at position -Y was the most significant. GPIIb 242–255 with only Tyr at position 11 gave a weak Tb^{3+} luminescence at 545 nm upon titration with $TbCl_3$. Incorporation of Tyr and Trp into positions -Y and 11, respectively, resulted in a 3.5-fold increase of Tb^{3+} luminescence (Figure 4A). Similarly, GPIIb 296–309(W) containing only a Trp substitution at position 11 was much less effective at enhancing Tb^{3+} luminescence than GPIIb 296–309(Y,W) with the additional Tyr at position -Y (Figure 4B). Therefore, in subsequent experiments, all of the GPIIb and GPIIIa

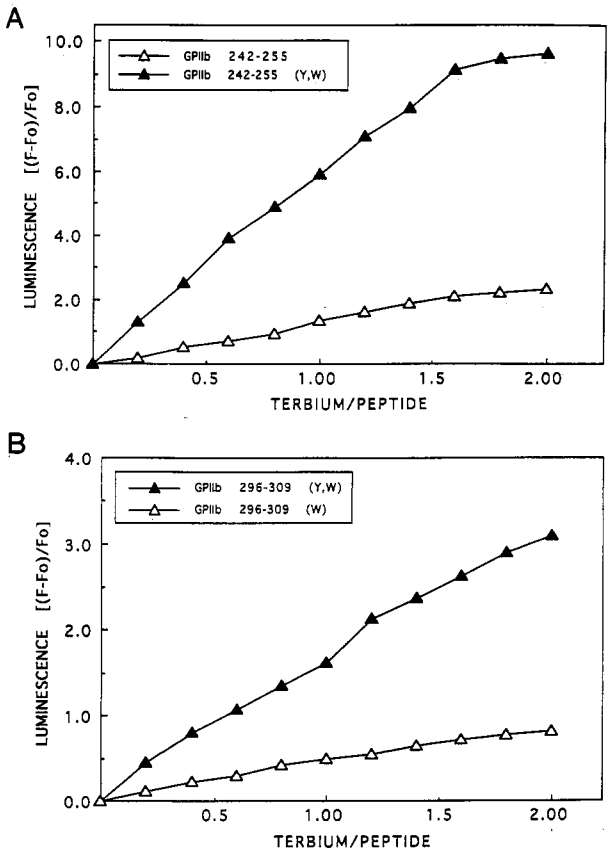

FIGURE 4: Effect of placement of aromatic amino acid donors on Tb^{3+} luminescence spectroscopy of GPIIb peptides. Panel A shows titration of peptide variants of GPIIb 242–255 with Tb^{3+}. The peptides contain either a single Tyr at position 11 (- △ -) or Trp and Tyr at positions 11 and -Y (- ▲ -), respectively, as energy donors to bound Tb^{3+}. Panel B shows Tb^{3+} luminescence of peptide variants of GPIIb 296–309 which have either a single Trp residue at position 11 (- △ -) or Trp and Tyr residues at positions 11 and -Y (- ▲ -), respectively. Tb^{3+} luminescence was measured at 545 nm, with excitation of the peptides at 285 nm. (Numbering begins with the first oxygenated residue in each peptide: Glu in peptides in panel A and Asp in peptides in panel B).

peptides used for Tb^{3+} luminescence studies contained both aromatic residues in the same positions.

Binding of Tb^{3+} to Synthetic GPIIb Peptides. Titration of all four synthetic peptides corresponding to the putative Ca^{2+}-binding motifs in GPIIb resulted in enhanced Tb^{3+} emission at 545 nm, indicating that the peptides were capable of binding metal ions. With each peptide, the luminescence reached a plateau at a 1.5–2.0/1.0 molar ratio of Tb^{3+} to peptide (Figure 5), and at this molar ratio, maximal quenching of the Trp donor was also observed (not shown). The peptides differed significantly in the efficiency of energy transfer to bound Tb^{3+}. Upon binding Tb^{3+}, GPIIb 296–309(Y,W) gave the lowest increase in Tb^{3+} luminescence, while GPIIb 425–438(W) yielded the highest emission. The order of efficiency of energy transfer from the aromatic donors within the GPIIb peptides to the bound Tb^{3+} is GPIIb 425–438(W) > GPIIb 242–255-(W) > GPIIb 364–377(W) > GPIIb 296–309(Y,W).

Binding of Tb^{3+} to the Synthetic GPIIIa Peptides. The saturation curves obtained upon titration of GPIIIa peptides with Tb^{3+} are shown in Figure 6. GPIIIa 118–131 was very effective at enhancing Tb^{3+} luminescence and gave a maximal emission at a molar ratio of 1.5 Tb^{3+}/peptide. At this ratio, maximal quenching of the Trp donor was also observed (not shown). Substitution of Ala in position 1 for Asp resulted in a marked (5-fold) reduction of Tb^{3+} luminescence, indicating

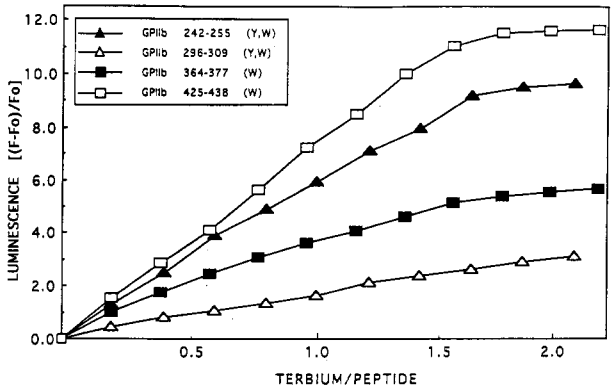

FIGURE 5: Terbium binding to the candidate cation-binding peptides from GPIIb. The four peptides are analogs of GPIIb 242–255 (- ▲ -), 296–309 (- △ -), 364–377 (- ■ -) and 425–438 (- □ -) and contain Tyr at position -Y and Trp at position 11 as potential energy donors to bound Tb^{3+}.

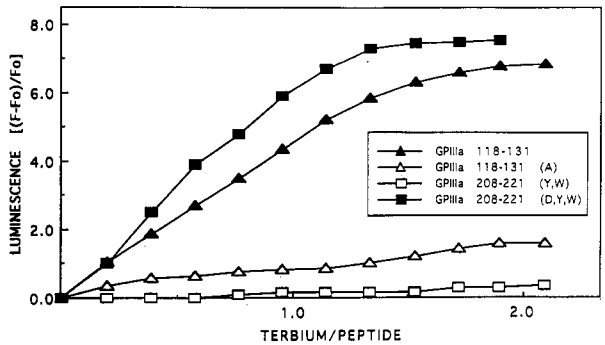

FIGURE 6: Terbium binding to the candidate cation-binding peptides from GPIIIa. The peptides are GPIIIa 118–131 (- ▲ -); a variant of this peptide in which Ala is substituted for the Asp at position X (- △ -), the first oxygenated coordination position; GPIIIa 208–221 with a Tyr at position 4 (- □ -); and a variant of this peptide in which Asp is substituted for the Lys at position X (- ■ -).

that the modified peptide had a significantly lower affinity for Tb^{3+} than GPIIIa 118–131. The importance of the Asp residue at position 1 for binding of Tb^{3+} was further evidenced by a lack of energy transfer in GPIIIa 208–221(Y,W). This peptide corresponds to the second candidate Ca^{2+}-binding site in GPIIIa. Although it contains the same coordinating residues as GPIIIa 118–131 at positions Y, Z, and -X and additionally has the preferred Glu residue at position -Z, no Tb^{3+} binding was detected. When Asp was substituted at position X to produce GPIIIa 208–221(D,Y,W), this peptide now bound Tb^{3+} and produced a very strong enhancement of Tb^{3+} luminescence (Figure 6).

Occupancy of the Metal-Binding Sites within GPIIb and GPIIIa Peptides by Divalent Cations. The binding constants of the various GPIIb and GPIIIa peptides for Tb^{3+}, Mn^{2+}, Ca^{2+}, and Mg^{2+} were derived from fluorescence measurements. In these experiments, Tb^{3+} (15 μM) and peptide (20 μM) were mixed, and the intensity of Tb^{3+} luminescence was recorded. Incremental amounts of competing ions were added, and the Tb^{3+} luminescence was again recorded. Displacement of Tb^{3+} bound to the various GPIIb and GPIIIa peptides by Mn^{2+} is shown in Figure 7. With each peptide, Mn^{2+} produced a dose-dependent reduction in Tb^{3+} luminescence. As this reduction in luminescence is directly proportional to the amount of Tb^{3+} displaced by the competing ion, relative binding constants could be derived. Furthermore, since the absolute value of the binding constant for Tb^{3+} could be determined from the fluorescence measurements, the absolute binding constant for each competing ion could also be

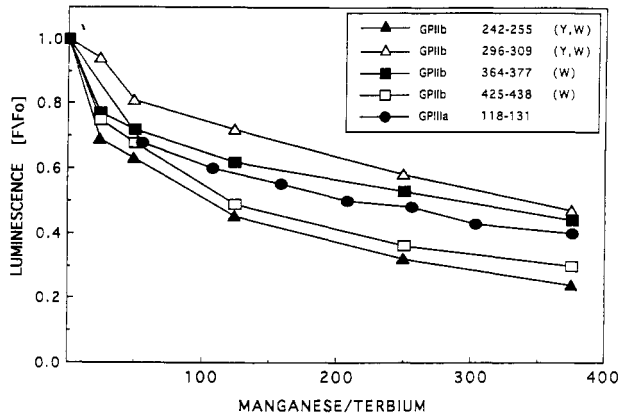

FIGURE 7: Displacement of Tb^{3+} bound to the various peptide fragments of GPIIb and GPIIIa by Mn^{2+}. Complexes of GPIIIa 118–131 (- ● -), GPIIb 242–255(Y,W) (- ▲ -), GPIIb 296–303(Y,W) (- △ -), GPIIb 364–377(W)(- ■ -), GPIIb 425–438(W) (- □ -) with Tb^{3+} (20 μM peptide and 15 μM $TbCl_3$) in 10 mM HEPES buffer, pH 7.3, were titrated with $MnCl_2$. Tb^{3+} luminescence was excited at 285 nm and measured at 545 nm.

Table 2: Binding Constants of Synthetic GPIIb-IIIa Peptide Loops for Cations

	affinity constants (K_a) (M^{-1})[a]			
peptides	Tb^{3+} ($\times 10^5$)	Mn^{2+} ($\times 10^2$)	Ca^{2+} ($\times 10^2$)	Mg^{2+} ($\times 10^2$)
GPIIb 242–255(Y,W)	2.56	9.84	6.14	3.84
GPIIb 296–309(Y,W)	0.67	2.16	0.73	
GPIIb 364–377(W)	2.32	6.27	2.78	
GPIIb 425–438(W)	2.38	10.8	3.10	2.35
GPIIIa 118–131	4.21	9.35	7.38	3.32

[a] Data represent mean values from three separate experiments. Standard deviations were less than 10% in all cases.

calculated. These values are summarized in Table 2. The affinity of Tb^{3+} for the synthetic peptides ranged from 6.7×10^4 to 4.2×10^5 M^{-1}. For the competing ions, Mn^{2+} had the highest affinities, and Mg^{2+}, the lowest affinities, for the various peptides. The binding constants for Mn^{2+} were still more than 2 orders of magnitude lower than those for Tb^{3+}. Ca^{2+} and Mg^{2+} had still lower affinities.

DISCUSSION

In this study, terbium luminescence spectroscopy has been utilized to characterize the interaction of metal ions with GPIIb-IIIa and short linear peptide segments from the receptor. The results support the following conclusions: (1) Tb^{3+} binds GPIIb-IIIa and supports the ligand binding function of the receptor. (2) Five cation binding sites with unequal affinities for Tb^{3+} can be demonstrated on the intact receptor. (3) The Tb^{3+}-binding sites are also capable of binding Ca^{2+} and Mn^{2+}, divalent cations which support ligand binding to the receptor. (4) Peptides corresponding to the four putative Ca^{2+}-binding sequences of GPIIb can, in fact, bind Tb^{3+} and divalent cations. (5) Of the two candidate sequences within GPIIIa, GPIIIa 118–131 appears to be a functional metal-binding site, whereas GPIIIa 208–221 does not. (6) The amino-terminal aspects of EF-hand-like structures appear to be particularly critical for metal binding function. These conclusions are discussed below.

The present study clearly shows that Tb^{3+} luminescence spectroscopy is a useful and facile probe of the metal-binding properties of GPIIb-IIIa. Tb^{3+} bound to the receptor, and the filling of these binding sites rendered the receptor competent to bind ligand. Moreover, the Tb^{3+}-binding sites could also be occupied by Ca^{2+}, Mg^{2+}, and Mn^{2+}, cations known to be relevant to the ligand-binding function of the receptor. On the basis of the Tb^{3+} titration curves with the intact receptor, GPIIb-IIIa appears to contain five metal-binding sites. The agreement of this conclusion with recently reported data in the literature appears to validate the luminescence technique. Using equilibrium dialysis, Rivas and Gonzalez-Rodríguez (1991) estimated that purified GPIIb-IIIa in Triton X-100 bound five Ca^{2+} ions; one site was high-affinity, and the other four sites were of lower affinity. In addition, in a preliminary study, Piotrowicz et al. (1991) utilized equilibrium gel filtration and *in situ* oxidation of cobalt to estimate the presence of five Co^{2+}-binding sites within the receptor. The agreement as to the presence of five metal-binding sites in the receptor by these diverse approaches does not exclude the existence of additional cation-binding sites, of either higher or lower affinity; however, the data do appear to indicate that the filling of one or more of the detected sites with Tb^{3+} or an appropriate divalent ion is necessary for the ligand-binding function of the receptor. The binding of Tb^{3+} to GPIIb-IIIa produced a sigmoidal curve of luminescence. The shape of this curve may indicate (a) a significantly lower quantum yield of Tb^{3+} luminescence from the site which binds the first Tb^{3+} than from the remaining sites or (b) cooperative Tb^{3+} binding among the five cation-binding sites. Mathematical modeling of the experimental data in Figure 2 did not discriminate these two possibilities; i.e., the fits of the data to these two possible models were not statistically different ($r^2 > 0.98$ for both models).

The results obtained with the intact receptor can be related to the primary sequence of GPIIb-IIIa. Sequence analysis suggests four possible Ca^{2+}-binding sites in GPIIb (Poncz et al., 1987), GPIIb 242–255, 296–309, 364–377, and 425–438, and two in GPIIIa, GPIIIa 118–131 and 208–222. Tb^{3+} luminescence spectroscopy of synthetic peptides corresponding to all six putative Ca^{2+}-binding sites was performed, and five of them (the four in GPIIb sites and one in GPIIIa) bound Tb^{3+}. The affinities of the five peptides were similar with K_a values ranging from 6.7×10^4 to 4.2×10^5 M^{-1}. These binding constants are consistent with those obtained for synthetic peptide loops of calmodulin (Borin et al., 1989; Buchta et al., 1986) and troponin C (Kanellis et al., 1983). Native peptides GIIb 242–255 and GIIb 296–309, in contrast to GIIb 364–377 and GIIb 425–438 do not contain tyrosine at position -Y. Introduction of a tyrosine at position -Y for energy transfer also could provide an oxygen ligand for cation binding in the EF-hand motif of these peptides. However, several proteins which do not contain an oxygen ligand at the -Y position (Strynadka & James, 1989) bind Ca^{2+} with high affinity. Moreover, we also found that GIIb 242–255 and GIIb 296–309 with the native residue at position -Y bound Tb^{3+} (albeit with low luminescence signals), and this binding could be displaced by divalent cations. Thus, binding of Ca^{2+} to these regions in the native protein would appear to be a justified conclusion. All five of the peptide sequences lack Glu at the 12 (-Z) position. Thus, these data indicate that the presence of Glu at position -Z in synthetic Ca^{2+}-binding loops is not critical for Tb^{3+} binding affinity. In contrast, GPIIIa 208–221, which does contain Glu at this position but lacks Asp at position X, showed no detectable binding of Tb^{3+}. Similarly, substitution of Ala for the Asp at position X of the binding loop in peptide GPIIIa 118–131 resulted in a dramatic decrease in Tb^{3+} luminescence. It is noteworthy that mutant GPIIb-IIIa with Tyr substituted for Asp at this position (GPIIIa 119) did not bind macromolecular or peptide ligands (Loftus

et al., 1990). Our experiments with GPIIIa 118–131(A) provide evidence that impaired ligand binding of the mutant GPIIb-IIIa could be due to the lack of cation binding to this region. It has also been shown that substitution of Ala for Asp at the homologous position in the β_1 subunit causes a loss in function (Takada et al., 1992). Thus, the cation-binding properties of this region are likely to be important for the function of other integrins as well.

Studies on the conformation of synthetic peptide loops in solution show that a lanthanide, especially the ones of ionic radius close to that of Ca^{2+}, fold the peptide into the same three-dimensional structure that exists in the intact protein (Gariepy et al., 1985; Marsden et al., 1989). We can assume, therefore, that all of the peptides in this study folded around the bound Tb^{3+} in a similar manner. The carboxylate group of Asp at position X of the EF-hand-like site of Ca^{2+}-binding proteins plays a prominent role in the binding of Ca^{2+} by providing a nidus around which the first six residues of the loop fold (Strynadka & James, 1989). The critical role of Asp at this position and the lack of an effect of Glu at position -Z for interaction of the peptide loops with Tb^{3+} support the hypothesis that, even in short peptides, the bend providing the cation-binding site resides in the amino-terminal segment and only the first nine residues of the loop are critical for function (Snyder et al., 1981; Borin et al., 1989). This interpretation is consistent with crystallographic studies of calmodulin (Snyder et al., 1981) which show that, in all binding sites, the Ca^{2+} ions are displaced from the center of the loop toward the amino-terminal helix of the helix–loop–helix domain (Babu et al., 1985).

Tb^{3+} luminescence of the synthetic peptides was significantly quenched in the presence of Mn^{2+}, Ca^{2+}, and Mg^{2+} ions. The binding constants for these cations, determined by competition binding experiments, are significantly lower than those found for Tb^{3+} but are consistent with data in the literature (Buchta et al., 1986). In general, the affinity of Tb^{3+} for a peptide ligand is always higher than that of divalent cations, due to the higher charge density (Brittain et al., 1976). Among divalent cations, Mn^{2+} has the highest binding affinity, usually 1 order of magnitude higher than that of Ca^{2+}, and Mg^{2+} had the lowest affinity for all synthetic peptides. There was no evidence for selectivity in binding of the synthetic peptide loops toward these cations. Therefore, selective binding of Ca^{2+} or Mg^{2+} to some of the integrin receptors and other proteins containing EF-hand-like sequences depends upon conformational contributions from the intact proteins which control the coordination geometry of the metal-binding sites (Strynadka & James, 1989).

The conclusion that peptide sequences in both subunits are functional metal-binding sites is consistent with observations in the literature. Binding of $^{45}Ca^{2+}$ ions to both subunits was demonstrated in blotting experiments (Fujimura & Phillips, 1983). In equilibrium dialysis experiments (Rivas & Gonzalez-Rodriguez, 1991), Ca^{2+} binding to both subunits was detected. Furthermore, Gulino et al. (1992) found two classes of Ca^{2+}-binding sites in recombinant GPIIb fragment 171–464. Of the five functional synthetic peptides tested, one contains Trp and Tyr (IIIa 118–131) and three sites contain Tyr (IIb 242–255, 364–377 and 425–438) directly within the peptide sequences. GPIIb 296–309 does not contain an aromatic residue within the Ca^{2+}-binding loop but does contain a Tyr located 10 residues from the center of the Ca^{2+}-binding site. In folded GPIIb-IIIa, this Tyr residue may be sufficiently close to a Tb^{3+} bound to this site to allow for energy transfer, albeit less efficient than when the aromatic residue resides directly in the loop. Accordingly, it can be speculated that Tb^{3+} binding to GPIIb 296–309 could give rise to the sigmoidal appearance of the luminescence curve as observed in Figure 2.

In conclusion, these studies show that GPIIb-IIIa contains five Tb^{3+}-binding sites which can be identified by Tb^{3+} luminescence spectroscopy of either intact receptor or synthetic peptide loops. These sites are localized in sequences in both subunits: GPIIb 242–255, 296–309, 364–377, and 425–438 and GPIIIa 118–131. The second EF-hand-like sequence present in GPIII 208–221 does not interact with Tb^{3+} and divalent cations because it lacks a critical Asp residue in position X of the binding loop. The five synthetic peptide loops are functional Ca^{2+}-binding sites despite their lack of a Glu residue in position -Z, and they exhibit binding affinities similar to those reported for complete Ca^{2+}-binding loops such as those present in calmodulin and troponin C. These peptides, however, do differ in the efficiency of energy transfer from aromatic residues to Tb^{3+} bound to the peptide loops. The validation of terbium luminescence spectroscopy of GPIIb-IIIa and its peptides should allow application of this approach to analyze the metal-binding properties of other integrins.

ACKNOWLEDGMENT

We wish to thank Mr. Timothy Burke for his technical assistance, and Ms. Jane Rein for the preparation of the manuscript.

REFERENCES

Babu, Y. S., Sack, J. S., Greenhough, T. J., Bugg, C. E., Means, A. R., & Cook, W. J. (1985) *Nature 315*, 37.

Bairoch, A. (1989) in *PROSITE: A dictionary of protein sites and patterns*, University of Geneva, Geneva.

Bajt, M. L., Ginsberg, M. H., Frelinger, A. L., III, Berndt, M. C., & Loftus, J. C. (1992) *J. Biol. Chem. 267*, 3789.

Borin, G., Ruzza, P., Rossi, M., Calderan, A., Marchiori, F., & Peggion, E. (1989) *Biopolymers 28*, 353.

Brass, L. F., Shattil, S. J., Kunicki, T. J., & Bennett, J. S. (1985) *J. Biol. Chem. 260*, 7875.

Brittain, H. G., Richardson, F. S., & Martin, R. B. (1976) *J. Am. Chem. Soc. 98*, 9255.

Buchta, R., Bondi, E., & Fridkin, M. (1986) *Int. J. Pept. Protein Res. 28*, 289.

Burroughs, S. E., Eisenman, G., & Horrocks, W. DeW., Jr. (1992) *Biophys. Chem. 42*, 249.

Fitzgerald, L. A., & Phillips, D. R. (1985) *J. Biol. Chem. 260*, 11366.

Fitzgerald, L. A., Steiner, B., Rall, S. C., Jr., Lo, S. S., & Phillips, D. R. (1987) *J. Biol. Chem. 262*, 3936.

Fujimura, K., & Phillips, D. R. (1983) *J. Biol. Chem. 258*, 10247.

Gariepy, J., Kay, L. E., Kuntz, I. D., Sykes, B. D., & Hodges, R. S. (1985) *Biochemistry 24*, 544.

Ginsberg, M. H., Lightsey, A. L., Kunicki, T. J., Kaufman, A., Marguerie, G. A., & Plow, E. F. (1986) *J. Clin. Invest. 78*, 1103.

Gross, M. D., Nelsestuen, G. L., & Kumar, R. (1987) *J. Biol. Chem. 262*, 6539.

Gulino, D., Boudignon, C., Zhang, L. Y., Concord, E., Rabiet, M. J., & Marguerie, G. (1992) *J. Biol. Chem. 267*, 1001.

Hogue, C. W. V., MacManus, J. P., Banville, D., & Szabo, A. G. (1992) *J. Biol. Chem. 267*, 13340.

Horrocks, W. DeW., Jr., & Sudnick, D. R. (1979) *J. Am. Chem. Soc. 101*, 334.

Horrocks, W. DeW., Jr., & Sudnick, D. R. (1981) *Acc. Chem. Res. 14*, 384.

Horrocks, W. DeW., Jr., & Albin, M. (1983) *Prog. Inorg. Chem. 31*, 1.
Hynes, R. O. (1987) *Cell 48*, 549.
Kanellis, P., Yang, J., Cheung, H. C., & Lenkinski, R. E. (1983) *Arch. Biochem. Biophys. 220*, 530.
Kirchhofer, D., Gailit, J., Ruoslahti, E., Grzesiak, J., & Pierschbacher, M. D. (1990) *J. Biol. Chem. 265*, 18525.
Laemmli, U. K. (1970) *Nature 227*, 680.
Lanza, F., Stierlé, A., Fournier, D., Morales, M., André, G., Nurden, A. T., & Cazenave, J.-P. (1992) *J. Clin. Invest. 89*, 1995.
Loftus, J. C., O'Toole, T. E., Plow, E. F., Glass, A., Frelinger, A. L., & Ginsberg, M. H. (1990) *Science 249*, 915.
Luk, C. K. (1971) *Biochemistry 10*, 2838.
MacManus, J. P., Hogue, C. H., Marsden, B. J., Sikorska, M., & Szabo, A. G. (1990) *J. Biol. Chem. 265*, 10358.
Malik, N. A., Anantharamaiah, G. M., Gawish, A., & Cheung, H. C. (1987) *Biochim. Biophys. Acta 911*, 221.
Marguerie, G. A., Edgington, T. S., & Plow, E. F. (1980) *J. Biol. Chem. 255*, 154.
Marsden, B. J., Hodges, R. S., & Sykes, B. D. (1989) *Biochemistry 28*, 8839.
Phillips, D. R., Charo, I. F., Parise, L. V., & Fitzgerald, L. A. (1988) *Blood 71*, 831.
Piotrowicz, R. S., Plow, E. F., & Smith, J. W. (1991) *Blood (Suppl.) 77*, 243A (Abstract).
Plow, E. F., & Ginsberg, M. H. (1989) in *Progress in Hemostasis and Thrombosis, Vol. 9* (Coller, B. S., Ed.) pp 117–156, W. B. Saunders, Philadelphia, PA.
Poncz, M., Eisman, R., Heidenreich, R., Silver, S. M., Vilaire, G., Surrey, S., Schwartz, E., & Bennett, J. S. (1987) *J. Biol. Chem. 262*, 8476.
Prados, R., Stadtherr, L. G., Donato, H., Jr., & Martin, R. B. (1974) *J. Inorg. Nucl. Chem. 36*, 689.
Pytela, R., Pierschbacher, M. D., Ginsberg, M. H., Plow, E. F., & Ruoslahti, E. (1986) *Science 231*, 1559.
Reuken, J. (1977) in *Calcium binding proteins and calcium function*, Elsevier/North-Holland, New York.
Rivas, G. A., & González-Rodríguez, J. (1991) *Biochem. J. 276*, 35.
Ruoslahti, E. (1991) *J. Clin. Invest. 87*, 1.
Smyth, S. S., Joneckis, C. C., & Parise, L. V. (1993) *Blood 81*, 2827.
Snyder, A. P., Sudnick, D. R., Arkle, V. K., & Horrocks, W. DeW., Jr. (1981) *Biochemistry 20*, 3334.
Steiner, B., Cousot, A., Trzeciak, A., Gillessen, D., & Hadvary, P. (1989) *J. Biol. Chem. 264*, 13102.
Steiner, B., Parise, L. V., Leung, B., & Phillips, D. R. (1991) *J. Biol. Chem. 266*, 14986.
Strynadka, N. C., & James, M. N. (1989) *Annu. Rev. Biochem. 58*, 951.
Takada, Y., Ylanne, J., Mandelman, D., Puzon, W., & Ginsberg, M. H. (1992) *J. Cell Biol. 119*, 913.
Tuckwell, D. S., Brass, A., & Humphries, M. J. (1992) *Biochem. J. 285*, 325.
van Sharrenberg, G. J. M., Slotbloom, A. J., de Haas, G. H., Mulqueen, P., Breen, P. J., & Horrocks, W. DeW., Jr. (1985) *Biochemistry 24*, 334.